

## Supporting Information

### **Hydrothermal Control of the lithium-rich $\text{Li}_2\text{MnO}_3$ phase in lithium manganese oxide nanocomposites and their application as precursors for lithium adsorbents**

Ruth Pulido<sup>a,b\*</sup>, Nelson Naveas<sup>a,b</sup>, Teófilo Graber<sup>b</sup>, Raúl J. Martín-Palma<sup>a</sup>, Fernando Agulló-Rueda<sup>c</sup>, Iván Brito<sup>d</sup>, Carlos Morales<sup>a</sup>, Leonardo Soriano<sup>a</sup>, Laura Pascual<sup>e</sup>, Carlo Marini<sup>f</sup>, Jacobo Hernández-Montelongo<sup>g</sup>, Miguel Manso Silván<sup>ah</sup>

<sup>a</sup>Departamento de Física Aplicada and Instituto Universitario de Ciencia de Materiales Nicolás Cabrera, Universidad Autónoma de Madrid, 28049 Madrid, Spain.

<sup>b</sup>Departamento de Ingeniería Química y Procesos de Minerales, Universidad de Antofagasta, Avenida Angamos 601, Antofagasta, Chile.

<sup>c</sup>Instituto de Ciencia de Materiales de Madrid (ICMM), CSIC, 28049 Madrid, Spain.

<sup>d</sup>Departamento de Química, Universidad de Antofagasta, Avda. Universidad de Antofagasta 02800, 1240000, Antofagasta, Chile.

<sup>e</sup>Instituto de Catálisis y Petroleoquímica, CSIC, 28049 Madrid, Spain.

<sup>f</sup>CELLS–ALBA Synchrotron, 08290 Cerdanyola del Valles, Spain.

<sup>g</sup>Departamento de Ciencias Matemáticas y Físicas, UC Temuco, 4813302 Temuco, Chile.

<sup>h</sup>Centro de Microanálisis de Materiales, Universidad Autónoma de Madrid, Campus de Cantoblanco, 28049 Madrid, Spain.

\*To whom correspondence should be addressed:

e-mail address: ruth.pulido@estudiante.uam.es

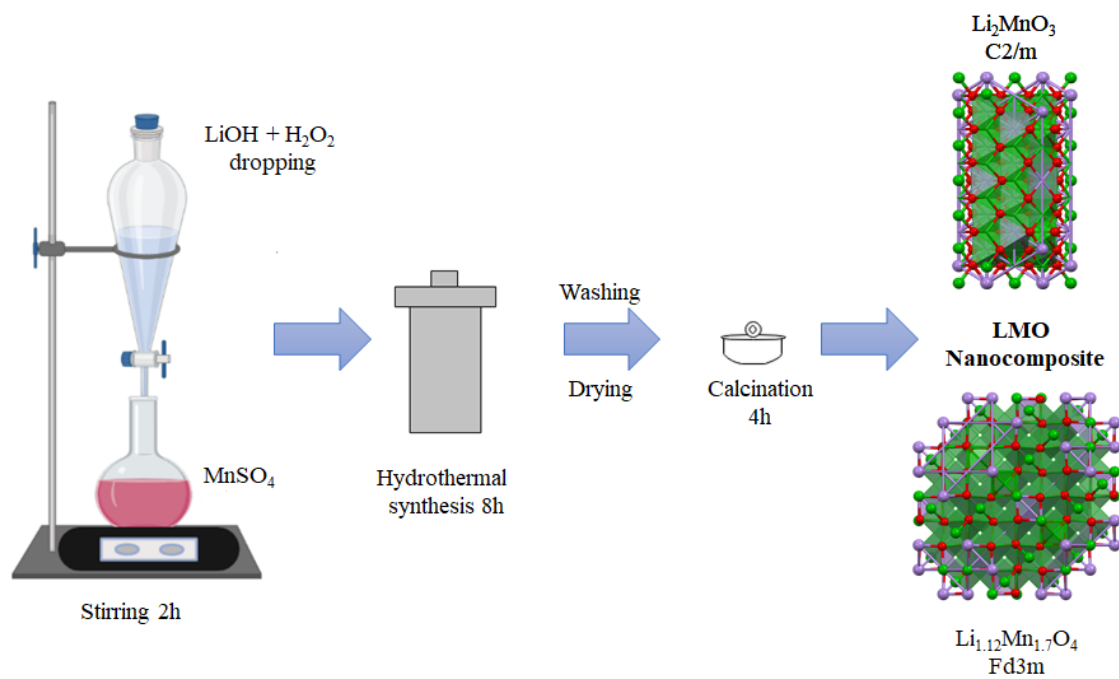


**Figure S1** Schematic representation of the hydrothermal synthesis of Li<sub>2</sub>MnO<sub>3</sub> · Li<sub>1.12</sub>Mn<sub>1.7</sub>O<sub>4</sub> nanocomposites.

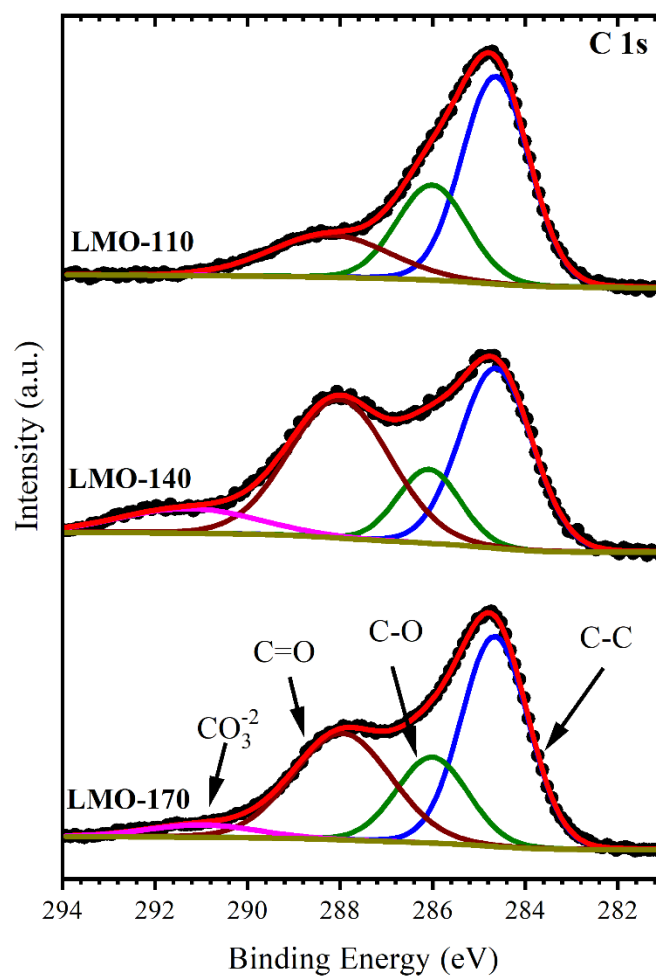


**Figure S2** High-resolution XPS spectra of C 1s from the LMO nanocomposites. The peak fitting analysis of C 1s core-level showed the typical C-C (284.60 eV) and C-O (286 eV) components. Moreover, around 288 and 291 eV, other two contributions can be assigned to C=O and CO<sub>3</sub><sup>-2</sup>-like, related to the adsorbed atmospheric carbon and further formation of Li<sub>2</sub>CO<sub>3</sub>, respectively<sup>1-4</sup>

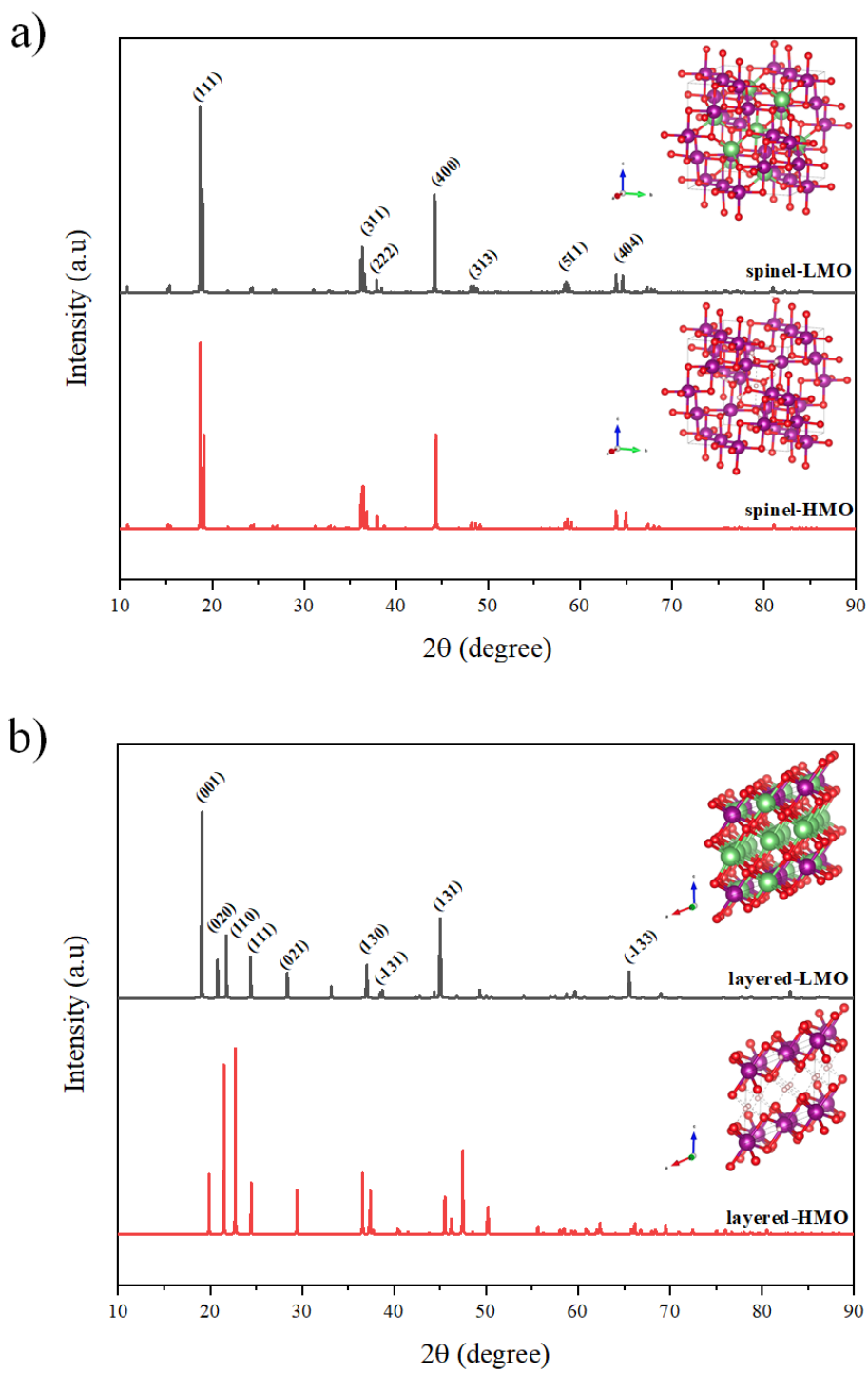


**Figure S3** Simulated XRD patterns of adsorbent precursor materials in pure phase.

Layered-LMO (a) and spinel-LMO (b).

**Table S1**

Structural parameters of LMO nanocomposites determined by Rietveld refinement of XRD data.

Nanocomposite	Phase	a (Å)	b (Å)	c (Å)	$\beta$ angle(°)	V (Å <sup>3</sup> )
LMO-110	Li <sub>1.12</sub> Mn <sub>1.7</sub> O <sub>4</sub>	8.1397	-	-	-	539.2955
	Li <sub>2</sub> MnO <sub>3</sub>	4.9400	8.5277	5.0085	108.800	199.7378
LMO-140	Li <sub>1.12</sub> Mn <sub>1.7</sub> O <sub>4</sub>	8.1272	-	-	-	536.8187
	Li <sub>2</sub> MnO <sub>3</sub>	4.9279	8.5260	5.0108	108.930	199.1424
LMO-170	Li <sub>1.12</sub> Mn <sub>1.7</sub> O <sub>4</sub>	8.1366	-	-	-	538.6697
	Li <sub>2</sub> MnO <sub>3</sub>	4.9303	8.5306	5.0130	108.943	199.4214

**Table S2**

Quantitative analysis C 1s XPS spectra of LMO nanocomposite

Sample	C-C%	C-O%	C=O%	CO <sub>3</sub> <sup>2-</sup> %
LMO-170	12.1	5.3	9.0	1.1
LMO-140	5.3	1.9	5.8	1.3
LMO-110	9.5	4.6	3.4	0.0

**Table S3**

DFT optimized cell parameters for simulated LMO and HMO

Structure	Cell parameters				
	a(Å)	b(Å)	c(Å)	$\beta$ angle (°)	Volume
Li <sub>9</sub> Mn <sub>15</sub> O <sub>32</sub>	8.19191	-	-	-	549.655156
H <sub>9</sub> Mn <sub>15</sub> O <sub>32</sub>	8.16750	-	-	-	544.333233
Li <sub>8</sub> Mn <sub>4</sub> O <sub>12</sub>	4.93214	8.53083	4.93276	109.5915	195.531518
H <sub>8</sub> Mn <sub>4</sub> O <sub>12</sub>	4.82884	8.92474	4.58778	115.7690	178.053829

**Table S4**

Simulated X-ray diffraction data for LMO and HMO

<i>hkl</i>	Li <sub>9</sub> Mn <sub>15</sub> O <sub>32</sub>		H <sub>9</sub> Mn <sub>15</sub> O <sub>32</sub>		Li <sub>8</sub> Mn <sub>4</sub> O <sub>12</sub>		H <sub>8</sub> Mn <sub>4</sub> O <sub>12</sub>	
	<i>d</i> (Å)	2 $\theta$	<i>d</i> (Å)	2 $\theta$	<i>d</i> (Å)	2 $\theta$	<i>d</i> (Å)	2 $\theta$
111	4.6822	18.93	4.5978	19.28	-	-	-	-
400	2.0477	44.19	2.0406	44.35	-	-	-	-
001	-	-	-	-	4.6471	19.08	4.1315	21.49
131	-	-	-	-	2.0107	45.05	1.9144	47.45

**References**

- 1 S.-H. Lee, I.-S. Jo and J. Kim, *Surf. Interface Anal.*, 2014, **46**, 570–576.
- 2 P. Verma, P. Maire and P. Novák, *Electrochim. Acta*, 2010, **55**, 6332–6341.
- 3 D. Aurbach, I. Weissman, A. Schechter and H. Cohen, *Langmuir*, 1996, **12**, 3991–4007.
- 4 L. El Ouatani, R. Dedryvère, J.-B. Ledeuil, C. Siret, P. Biensan, J. Desbrières and D. Gonbeau, *J. Power Sources*, 2009, **189**, 72–80.